Supplementary information

Non-fullerene all small molecule solar cell constructed with a diketopyrrolopyrrole-based acceptor having power conversion efficiency higher than 9% and energy loss of 0.54 eV

María Privado,[a] Pilar de la Cruz,[a] Subhayan Biswas,[b] Rahul Singhal,[c] Ganesh D. Sharma*[b] and Fernando Langa*[a]

[a] Universidad de Castilla-La Mancha, Institute of Nanoscience, Nanotechnology and Molecular Materials (INAMOL), Campus de la Fábrica de Armas, 45071-Toledo, Spain

[b] Department of Physics, The LNM Institute of Information Technology (Deemed University), Jamdoli, Jaipur (Raj.) 302031, India

[c] Department of Physics, Malviya National Institute of Technology, Jaipur (Raj.), India

1. General Remarks.

Experimental conditions. Anhydrous solvents were dried by purification system Pure-Sov 400. Chromatographic purifications were performed using silica gel 60 Merk 230-400 mesh ASTM. Analytical thin-layer chromatography was performed using ALUGRAM ® SIL G/UV_{254} silica gel 60. Nuclear magnetic resonance ^{1}H NMR and ^{13}C NMR were performed using Bruker Innova 400 Hz. Chemical shifts (δ) values are denoted in ppm. Residual solvent peaks being used as the internal standard ($CHCl_3$; δ = 7.27 ppm). ^{13}C NMR chemical shifts are reported relative to the solvent residual peaks ($CDCl_3$, δ = 77.00 ppm). MALDI-TOF spectra were obtained in VOYAGER DETM STR spectrometry, using Dithranol [1,8-dihydroxy-9(10H)-anthracenone] as matrix. Fourier transform infrared spectrophotometer (FT-IR) Thermo Nicolet AVATAR 370 was used with KBr method, in each case the most characteristic bands are indicated for each compound. Absorption spectra were performed on Shimadzu UV 3600 spectrophotometer. Solutions of different concentration were prepared in CH_2Cl_2, spectroscopy grade, with absorbance between 0.5 and 0.7 using a 1 cm UV cuvette. The thermal stability was evaluated by TGA on a Mettler Toledo TGA/DSC Start^{e} System under nitrogen, with a heating rate of 10 ºC/min.

Electrochemical Measurements: Reduction (E_{red}) and oxidation potentials (E_{ox}) were measured by cyclic voltammetry with a potentiostat BAS CV50W in a conventional three-electrode cell equipped with a glassy carbon working electrode, a platinum wire counter electrode, and an $Ag/AgNO_3$ reference electrode at scan rate of 100 mV/s. The E_{red} and E_{ox} were expressed vs. Fc/Fc^{+} used as external reference. In each case, the measurements were done in a deaerated solution containing 1 mM of a the sample compound in 0.1 M of $(n\text{-}Bu)_4NClO_4$ in *o*-DCB:Acetonitrile (4:1) as an electrolyte solution.

Computational Details: Theoretical calculations were carried out within the density functional theory (DFT) framework by using the Gaussian 09,[1] applying density functional theory at the

[1] Gaussian 09, Revision A.1, M. J. Frisch, G. W. Trucks, H. B. Schlegel, G. E. Scuseria, M. A. Robb, J. R. Cheeseman, G. Scalmani, V. Barone, B. Mennucci, G. A. Petersson, H. Nakatsuji, M. Caricato, X. Li, H. P. Hratchian, A. F. Izmaylov, J. Bloino, G. Zheng, J. L. Sonnenberg, M. Hada, M. Ehara, K. Toyota, R. Fukuda, J. Hasegawa, M. Ishida, T. Nakajima, Y. Honda, O. Kitao, H. Nakai, T. Vreven, J. A. Montgomery, Jr., J. E. Peralta, F. Ogliaro, M. Bearpark, J. J. Heyd, E. Brothers, K. N. Kudin, V. N. Staroverov, R. Kobayashi, J. Normand, K. Raghavachari, A. Rendell, J. C.

B3LYP level. The basis set of 6-31G* was used in the calculations (Supercomputation Service of UCLM).

2. ^{1}H NMR, ^{13}C NMR, FT-IR and MALDI-TOF spectra

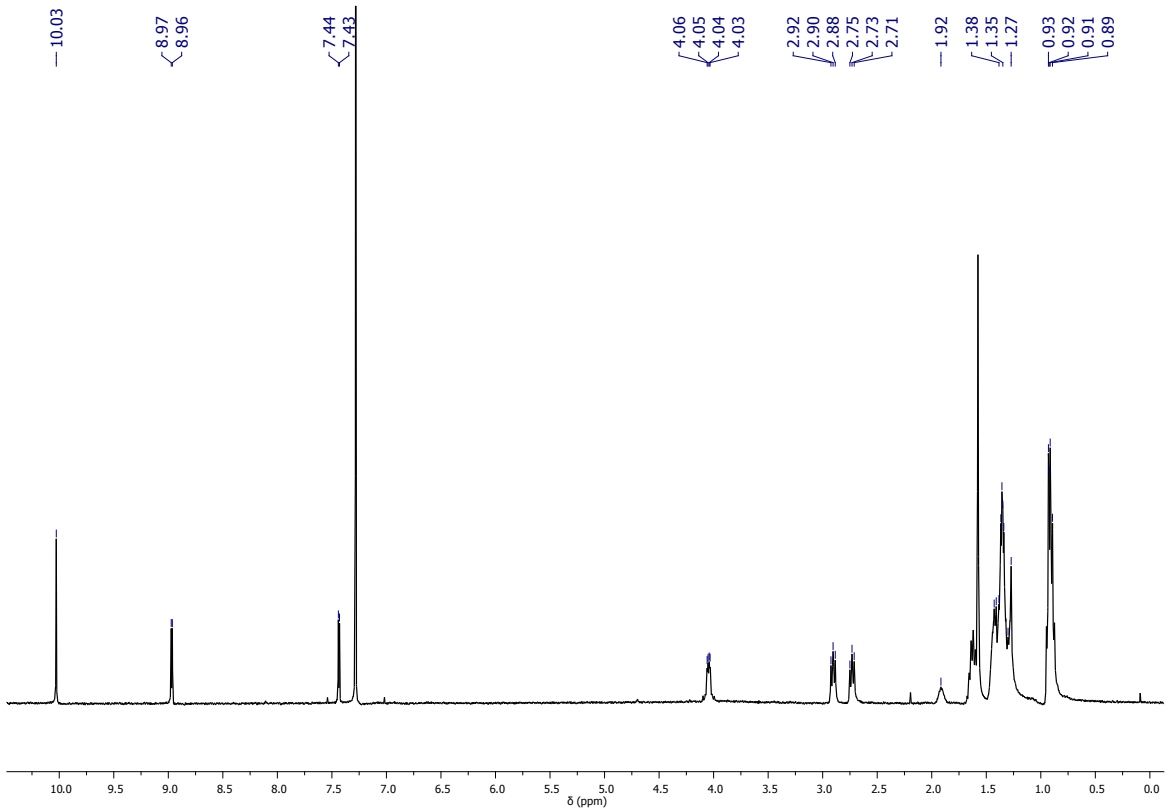

Figure S1. ^{1}H NMR of compound **3** (400 MHz, $CDCl_3$).

Burant, S. S. Iyengar, J. Tomasi, M. Cossi, N. Rega, J. M. Millam, M. Klene, J. E. Knox, J. B. Cross, V. Bakken, C. Adamo, J. Jaramillo, R. Gomperts, R. E. Stratmann, O. Yazyev, A. J. Austin, R. Cammi, C. Pomelli, J. W. Ochterski, R. L. Martin, K. Morokuma, V. G. Zakrzewski, G. A. Voth, P. Salvador, J. J. Dannenberg, S. Dapprich, A. D. Daniels, O. Farkas, J. B. Foresman, J. V. Ortiz, J. Cioslowski, and D. J. Fox, Gaussian, Inc., Wallingford CT, 2009.

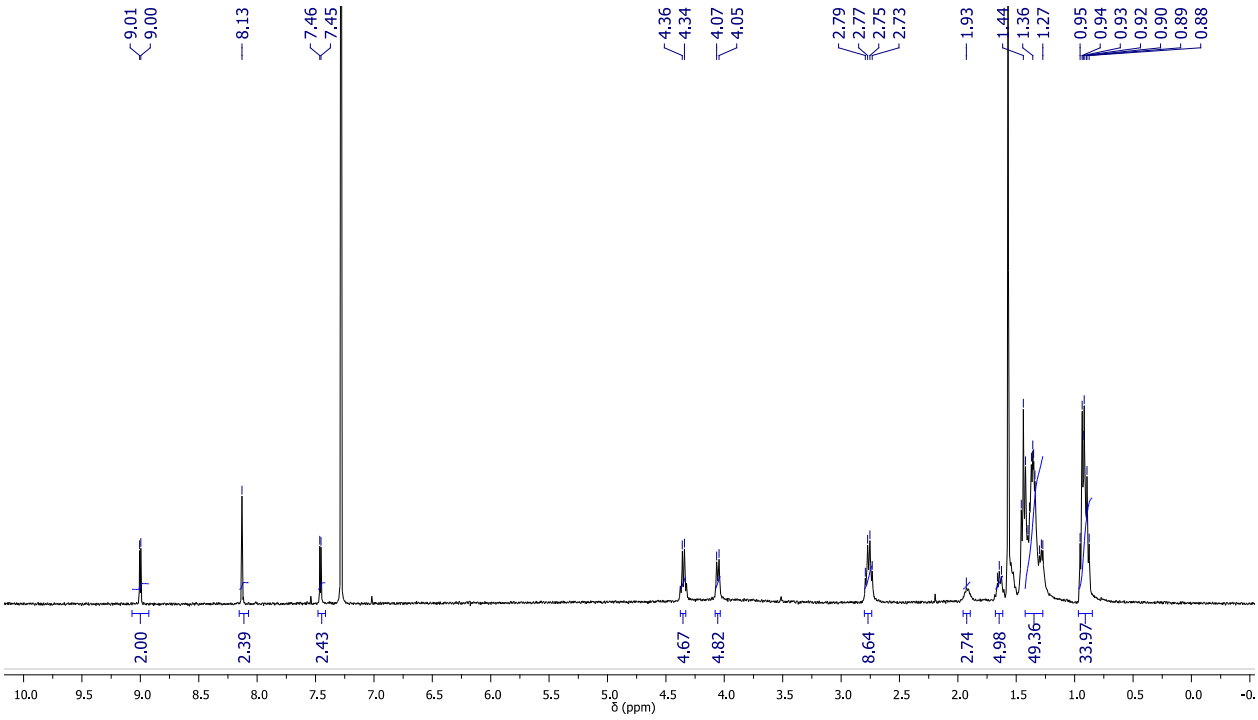

Figure S2. ^{1}H NMR of **MPU3** (400 MHz, $CDCl_3$).

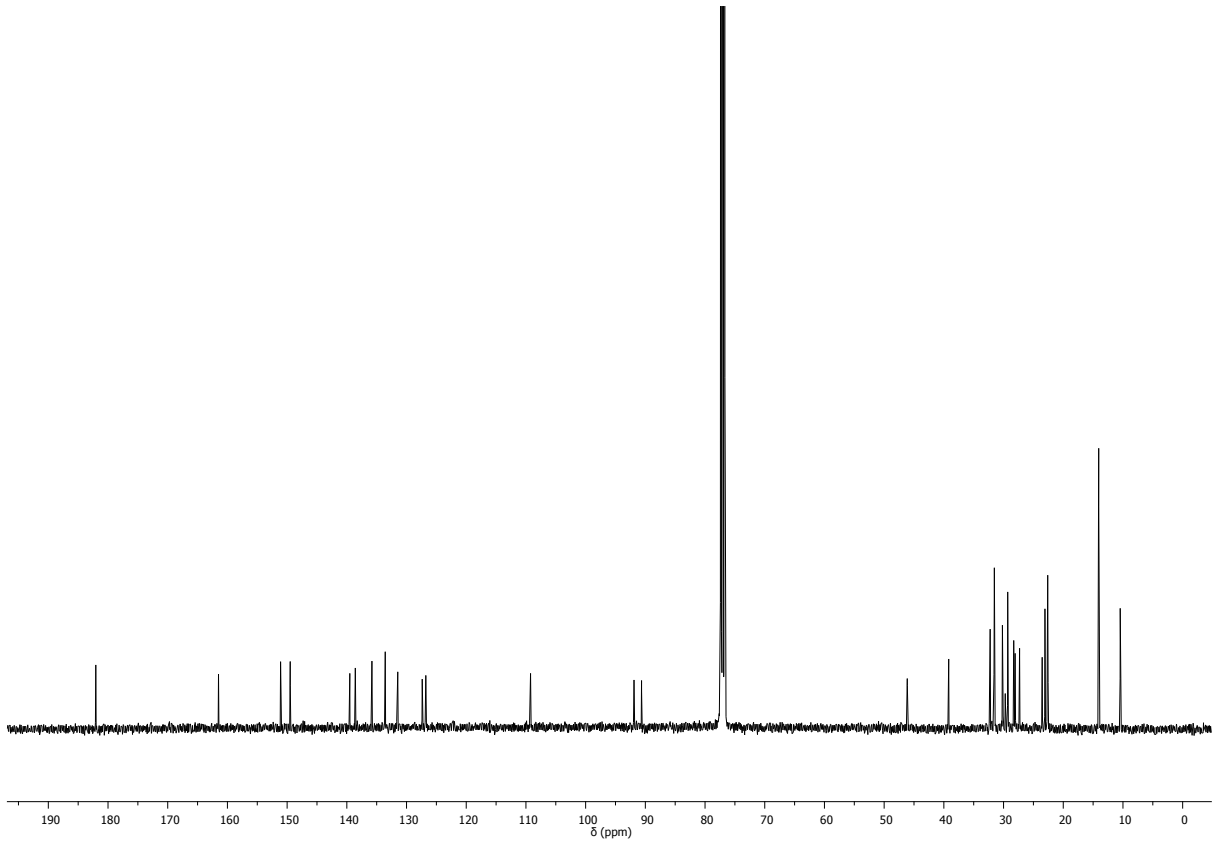

Figure S3. ^{13}C NMR of compound **3** (100 MHz, $CDCl_3$).

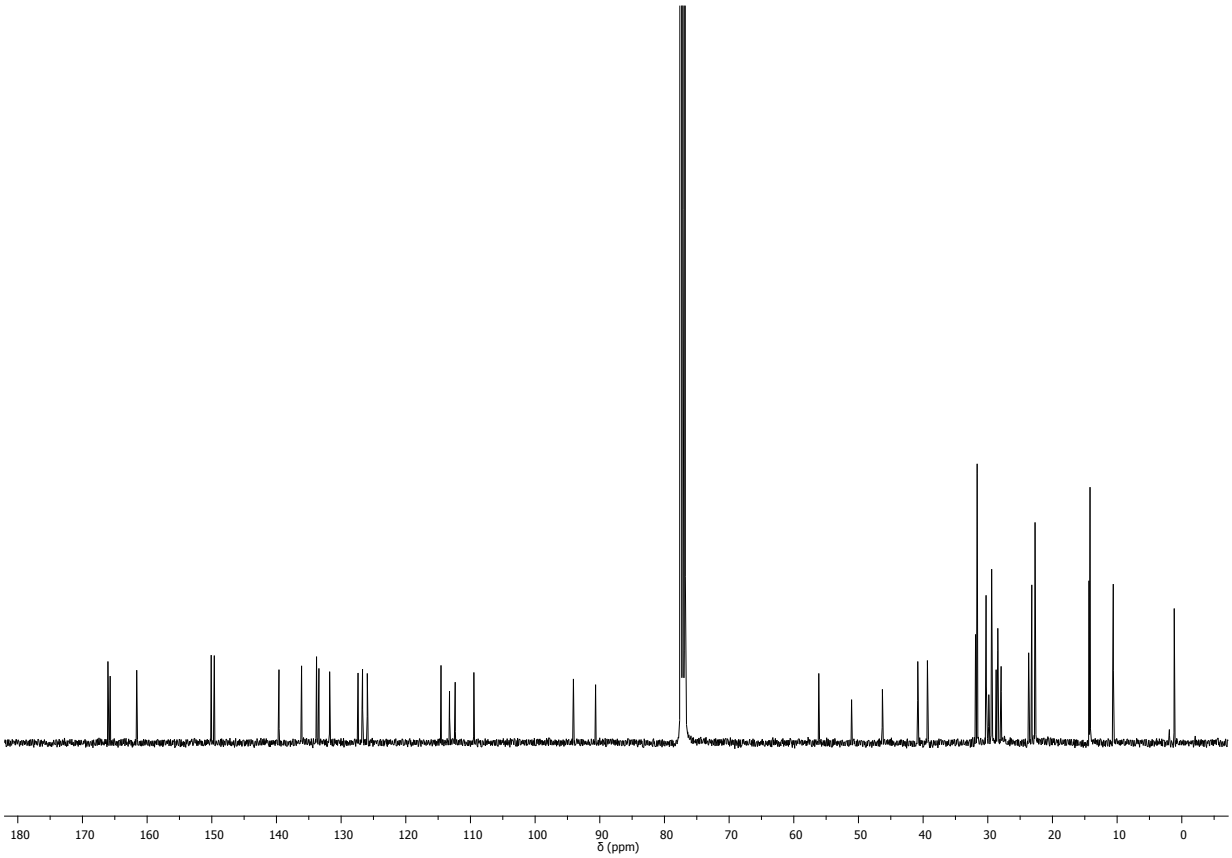

Figure S4. ^{13}C NMR of **MPU3** (100 MHz, $CDCl_3$).

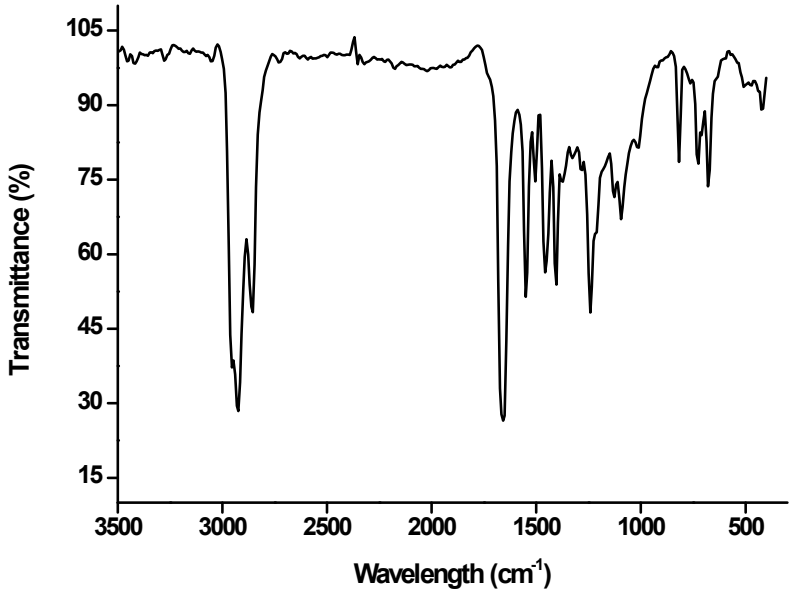

Figure S5. FT-IR (KBr) of compound **3**.

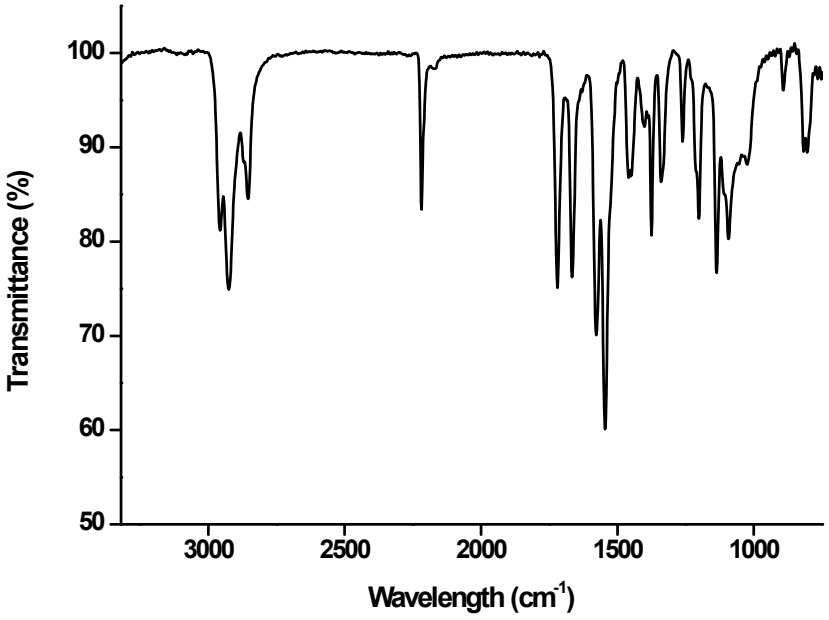

Figure S6. FT-IR (KBr) of **MPU3**.

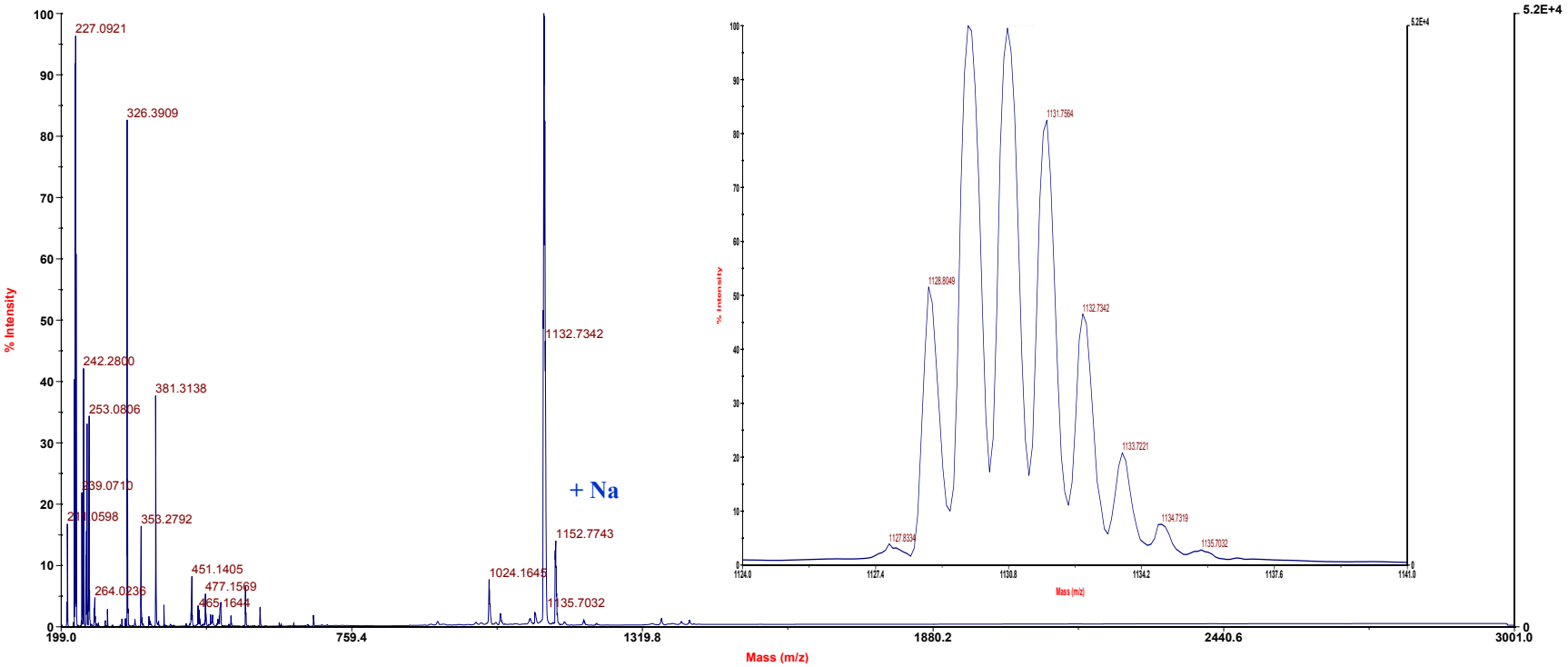

Figure S7. MALDI-TOF MS spectrum of compound **3** (Matrix: Dithranol).

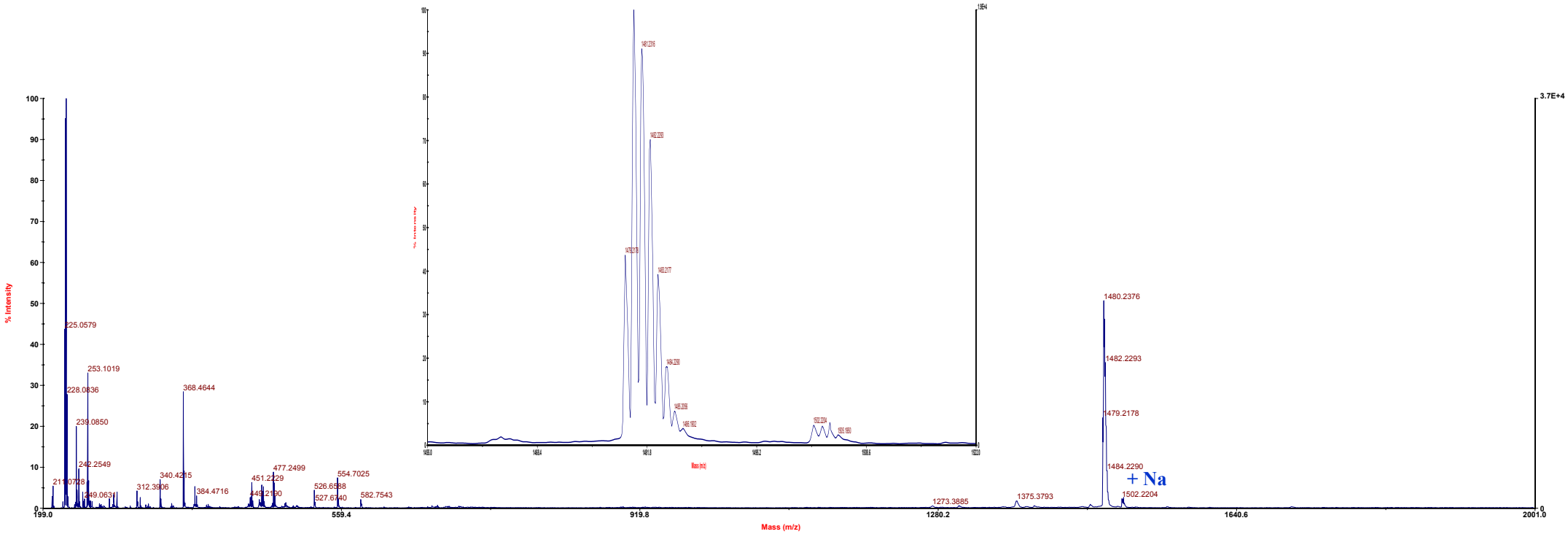

Figure S8. MALDI-TOF MS spectrum of **MPU3** (Matrix: Dithranol).

3. Thermogravimetric Analysis (TGA) and Differential Scanning Calorimetry (DSC) of MPU3

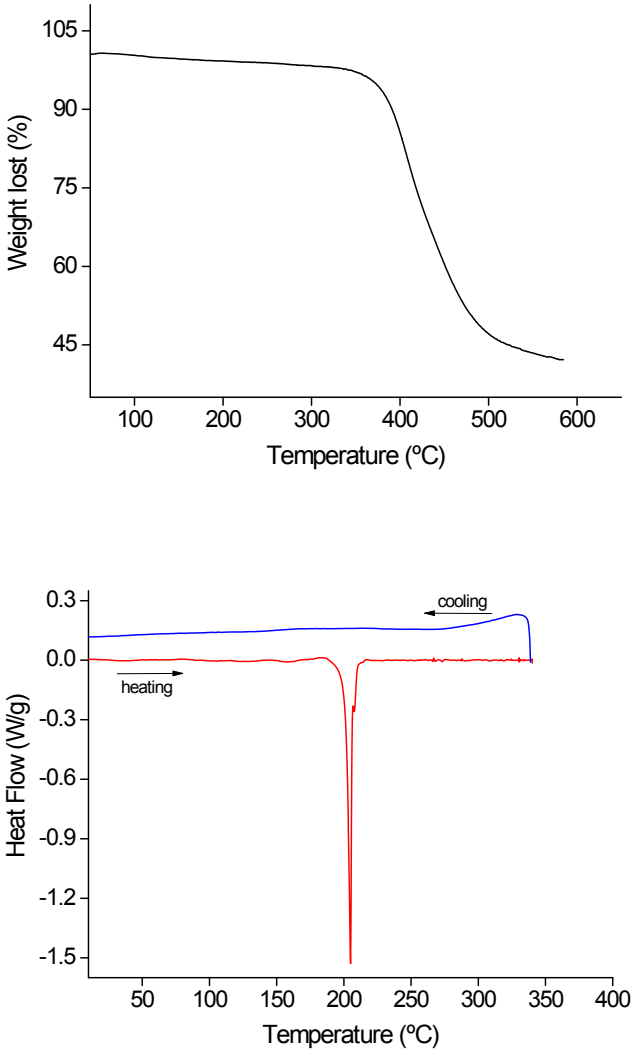

Figure S9. TGA (top) and DSC (bottom) curves of **MPU3**.

4. Absorption spectrum in solution

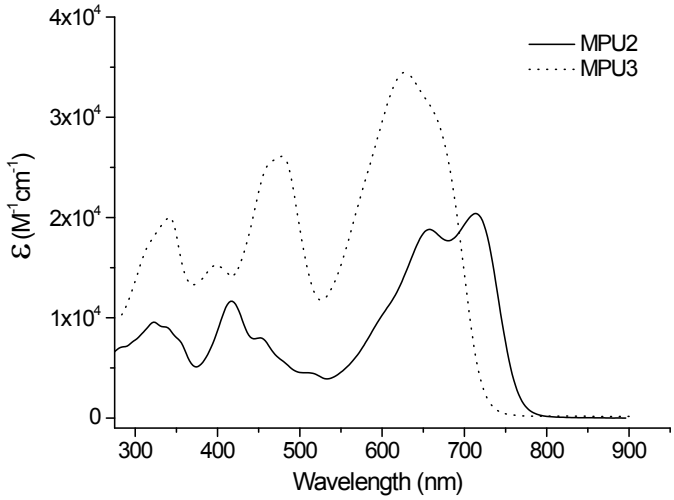

Figure S10. Absorption spectra, in CH_2Cl_2, of **MPU2** and **MPU3**.

5. Electrochemical Studies

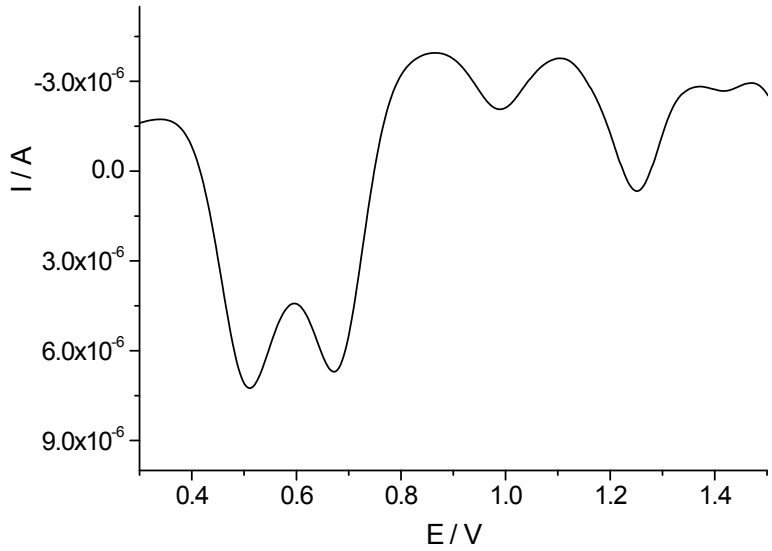

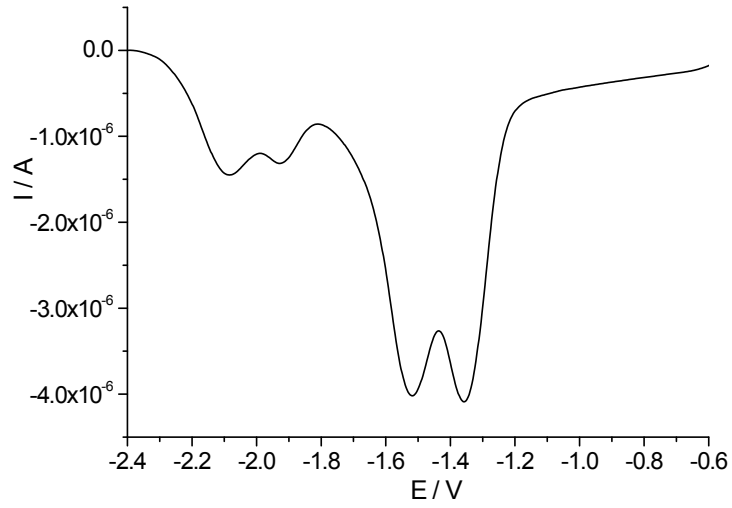

Figure S11. Osteryoung square wave voltammetries of **MPU3**: oxidation (top) and reduction (bottom).

6. Theoretical calculations

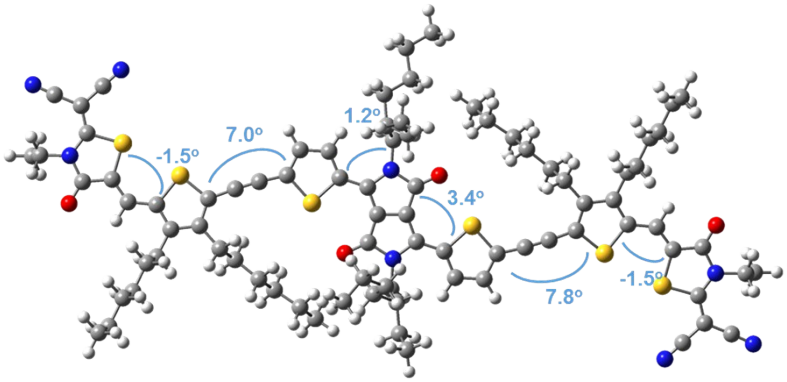

Figure S12. Theoretical optimized geometry and dihedral angles of **MPU3** (Gaussian 09W, DFT-B3LYP 6-31G*).